Hydrol. Earth Syst. Sci. Discuss., 7, 5213–5234, 2010
www.hydrol-earth-syst-sci-discuss.net/7/5213/2010/
doi:10.5194/hessd-7-5213-2010

Hydrology and
Earth System
Sciences
Discussions

Stemflow of desert shrub and its significance in soil moisture replenishment

X.-P. Wang[1,2], Z.-N. Wang[1], R. Berndtsson[2], Y.-F. Zhang[1], and Y.-X. Pan[1]

[1]Shapotou Desert Research and Experiment Station, Cold and Arid Regions Environmental and Engineering Research Institute, Chinese Academy of Sciences, Lanzhou 730000, China
[2]Department of Water Resources Engineering, Lund University, 22100 Lund, Sweden

Received: 27 March 2010 – Accepted: 12 July 2010 – Published: 2 August 2010

Correspondence to: X.-P. Wang (xpwang@lzb.ac.cn)

Published by Copernicus Publications on behalf of the European Geosciences Union.

Abstract

Stemflow of xerophytic shrubs represents a significant component of water replenishment to the soil-root systems influences water utilization of plant roots at the stand scale, especially for water scarce desert ecosystems. In this study, stemflow of *Caragana korshinskii* was quantified by aluminum foil collar collection method at revegetated sand dunes of the Shapotou restored desert ecosystem in Northwestern China. Meanwhile, time domain reflectometry probes were inserted horizontally at 20 different soil profile depths under the *C. korshinskii* shrub to monitor soil moisture variation at hourly intervals. Results indicated that 2.2 mm precipitation were necessary for the generation of stemflow for *C. korshinskii*. Stemflow averaged 8% of the gross precipitation, and the average funneling ratio was as high as 90. The soil moisture in the uppermost soil profile was strongly correlated with individual rainfall and the stemflow strengthened this relationship. Therefore, it is favorable for infiltrated water redistribution in the deeper soil profile of the root zone. We conclude that stemflow contributes significantly to a positive soil moisture balance in the root zone and the replenishment of soil moisture at deeper soil layers. This plays an important role in plant survival and the general ecology of arid desert environments.

1 Introduction

Water scarcity is greatest in semiarid and arid regions because of limited supplies and increasing demand due to greater population growth relative to more humid regions (Vörösmarty et al., 2000). Thus, precipitation plays an important role in water-scarce arid environments. The patterns of transferring limited rainfall to the soil will regulate the soil water replenishment and utilization of plant roots. Stemflow can concentrate the rainfall intercepted by leaves and branches to the plant stem. Since water resources are limited in arid lands, stemflow can be an important source of soil moisture replenishment in arid and semiarid lands (Tromble, 1987). Návar and Bryan (1990) calculated that stemflow input to the soil area around three semiarid shrub stems in Northeastern Mexico represented a water input that was five times by other areas below the shrub canopies. Other arid shrubs are also adapted to divert rainfall to the base of their stems as stemflow where it subsequently infiltrates the soil and remains available for plant uptake at deeper soil layers (Pressland, 1976; Nulsen et al., 1986; Návar, 1993; Martinez-Meza and Whitford, 1996; Li et al., 2008). Levia and Frost (2003) provided a thorough review of the quantitative and qualitative importance of stemflow in forests as well as in agricultural environments.

Herwitz (1986) suggested that the quantitative importance of stemflow at the point scale can be expressed as a funneling ratio, F:

$$F = \frac{\mathrm{SF}}{\mathrm{BA} \times P} \tag{1}$$

where SF is the volume (l) of stemflow, BA is the trunk basal area (m^2), and P is the depth equivalent of gross incident precipitation (mm). The product BA×P provides the volume of water that would have been caught by a rain gauge having an opening equal to that of the trunk basal area. Thus, F represents the ratio of the amount of precipitation delivered to the base of the shrubs to the rainfall that would have reached the ground if the shrub were not present. Many studies in arid environments indicate that funneling ratio can be $>$10 and in some cases $\gg$10 (e.g. Návar, 1993; Carlyle-Moses, 2004; Li, et al., 2008). Consequently, the water volume that enters the soil around the stem will be greater than that under the corresponding rainfall due to the high funneling ratio.

Re-vegetation experiments have been established for more than 50 years in the southeastern fringe of the Tengger Desert, using mainly xerophytic shrubs, such as *C. korshinskii, Hedysarum scoparium* and *Artemisia ordosica*. The low water content of desert soils limits the number of shrubs and its stabilization. The effects of both rainfall and soil surface characteristics on soil water replenishment in the revegetated desert ecosystems have been studied by Wang et al. (2007, 2008). However, the effect of stemflow on infiltration patterns associated with the soil moisture replenishment is almost totally unexplored.

The objectives of the study were to quantify the variation of stemflow of *C. korshinskii*, and to evaluate the stemflow water infiltration process in the re-vegetation stabilized semiarid shrub desert in Northwestern China that has changed from a bare to a vegetated soil. In the following chapter observations and methods are outlined. Then results from the stemflow observations are described. We close with a discussion of practical results and possibilities for scaling up of results.

2 Materials and methods

2.1 Study site description

The study was conducted at Shapotou Desert Research and Experiment Station (37°27′ N, 104°57′ E, 1339 m a.m.s.l.) on the southeastern fringe of the Tengger Desert, where successful revegetation experiments have been carried out since 1956 using a combination of windbreaks, straw checkerboard barriers, and planted xerophytic shrubs. The natural climatic conditions have been described in detail by Wang et al. (2004). Based on analysis of 50-year time series of meteorological data collected at the Shapotou Desert Research and Experiment Station, operated by the Chinese Academy of Sciences, precipitation is the only source of soil water in this area. Mean annual precipitation is 191 mm and about 80% of this fall between June and September, with a coefficient of variation as high as 46%. The annual potential evaporation is about 3000 mm. Mean daily temperature of the coldest month (January) is –6.1 °C and that of the warmest month (July) is 24.7 °C. Mean relative humidity varies from 31% (April) to 54% (August). The first frost occurs in late September and the last frost ends in mid-April. The area has large and dense reticulate dune chains. The main dune crest migrates southeastward at a velocity of 0.3–0.6 $\mathrm{m\,yr^{-1}}$. The dune sand consists of 99.7% fine sand with grain size between 0.05 and 0.25 mm, 0.1% of silt with grain size between 0.002 and 0.05 mm, and 0.2% of clay with grain size less than 0.002 mm (Wang et al., 2008). The soil is loose and impoverished mobile sand with a consistent moisture content ranging from 3–4% and classified as Typic Psammaquent (Berndtsson et al., 1996). The depth to groundwater is between 50 and 80 m and, therefore, is unable to support the natural vegetation.

2.2 Experimental set-up and data collection

Stemflow was measured for eight fully mature plants of 20-year-old *C. korshinskii* that was replanted in 1989 as 1-year-old seedlings in the water balance experimental field of Shapotou. The number, length, height, diameter of the branches was measured, and branch-angle was calculated by the branch height from the ground surface to the tip of the branch vertically and the distance of the branch away from the stem horizontally, the stem basal area in Eq. (1) is the sum of the basal area of each branch. Shrub canopy projective area was calculated by taking the longest and shortest diameters through the centre of the fullest part of the canopy (Table 1). For the stemflow collection, fine sandpapers were used to burnish the selected branch surface about 10 cm above ground. Then stemflow was collected using collars constructed from flexible aluminum foil plates that were fitted around the entire circumference of the branches. Each collar was sealed to the branch using all weather silicon caulking. Stemflow water was delivered from the collar to a collection bottle via a 1.5 cm aperture plastic hose (Fig. 1). Stemflow was measured by graduated cylinder for each branch after each rainfall event and summarized for a single shrub. Stemflow volume of each shrub was divided by its canopy area to calculate the stemflow depth on a stand basis. The stemflow measurements under natural rainfall conditions was carried out according to Dunkerley's (2008) standard for identifying individual rainfall events in accordance with the condition of dry desert environments in Shapotou, where an individual rainfall event was defined as a rainfall separated by dry intervals of at least 6 h.

For measuring the soil moisture, time domain reflectometry (TDR) probes (Model 6050X1, Trase System I, Soilmoisture Equipment Corp., USA) were inserted at twenty depths of 5, 10, 15, 20, 25, 30, 35, 40, 45, 50, 60, 70, 80, 90, 100, 120, 140, 160, 180, and 200 cm. The probe has three 20 cm rods spaced 2.5 cm apart. For probe installation, a pit, 20 cm away from the stem, was dug in the soil of sufficient width to be able to insert the probes. The probes were inserted into the soil through the side of the pit that was unaltered and were placed horizontally in the direction of the shrub site. Once the probes had been inserted, the pit was carefully refilled, avoiding perturbations as far as possible, and the surface was contoured similar to the surrounding slope. To reduce the influence of terrain, shrubs of *C. korshinskii* growing at a flat ground were selected. The experiment was set up in February 2008, and soil moisture measurements associated with the stemflow measurements were done between July and October 2008.

The TDR instrument is capable of measuring volumetric soil moisture between 0% and 100%, with an accuracy of ≤0.1%. The wetting front location and cumulative infiltration are detected by measuring changes in soil moisture in the soil profile (Noborio et al., 1996; Wang et al., 2007). Noborio et al. (1996) found that the cumulative infiltration estimated by TDR compared favourably with observed infiltration, and the distance to the wetting front from the soil surface estimated by TDR agreed well with the observed values. All data were collected simultaneously during and directly following rain events sufficient to trace wetting front changes at hourly intervals.

According to the above, volumetric soil water content was measured with TDR probes matching the different depth of the soil profiles. Hence, water balances can be calculated according to the position of TDR probes. Based on the principle of soil water balance, the cumulative infiltration can be described as:

$$I = 10(\theta_e - \theta_\mathrm{i})Z_f \qquad (2)$$

$$\Delta S = \sum_{d=1}^{20} I_\mathrm{d} \qquad (3)$$

where θ_e is the volumetric soil water content ($\mathrm{cm}^3\,\mathrm{cm}^{-3}$), θ_i is initial volumetric soil water content ($\mathrm{cm^3\,cm^{-3}}$), Z_f is infiltration depth (mm), ΔS the soil moisture increment (mm), and I_d is cumulative infiltration at a specific depth section (mm).

A standard automatic rain gauge with a resolution of 0.1 mm (Adolf Thies GMVH & Co. KG, Germany) was installed at an open area 50 m away from the study plot, to obtain the amount and intensity of rainfall.

3 Results

3.1 Rainfall characteristics during the experiment period

There were totally 41 rainfall events in the year 2008, resulting in an annual rainfall of 127.8 mm with an average event rainfall intensity of 1.5 $\mathrm{mm\,h^{-1}}$ ranging from 0.2 to 14.7 $\mathrm{mm\,h^{-1}}$, and an average individual rainfall of 3.1 mm ranging from 0.1 to 21.6 mm (Fig. 2). There was no rainfall in March, May, November and December 2008 and it was a relatively dry year compared to the long-term average rainfall of 191 mm. Stemflow was monitored during a total of 14 rainfall events among the 41 rainfall events numbered 15, 16, 20, 22, 23, 24, 26, 27, 28, 32, 35, 36, 37, and 40 in Fig. 2, corresponding to the date of 13, 17, 30–31 July, 6, 8, 9, 26, 28, 28–29 August, 8, 22–23, 26–27 September, and 3, 21–22 October 2008. The 14 events produced a total of 87.8 mm rainfall, which accounted for 69% of the annual rainfall amount and 34% in events numbers (Fig. 2), which consisted of the main rain events ranging between 1.7 and 21.6 mm of the year 2008. The maximum rainfall intensity in 10 min (I_{10}) was 33 $\mathrm{mm\,h^{-1}}$, and the mean rainfall intensity ranged from 0.5 to 14.7 $\mathrm{mm\,h^{-1}}$ (Fig. 2). On the contrary, there were 23 rain events that accounted for 56% in events number contributed to less than 10% of the annual rainfall amount (12.3 mm in total) with no stemflow occurring. Note that the rainfall event numbered 34 occurred on midnight of 21 September at 22:50 LT till 22 September at 16:30 LT. This event had a rain depth of 15.6 mm was excluded from the analysis because the collect bottles overflowed before data collection. There are no indications that observed rainfall during the experimental period was not typical for the area. Thus, the observations in the present study are relevant to the estimation of stemflow and ratio to rainfall and likely representative for larger areas of the present.

3.2 Stemflow properties

Stemflow increased approximately linearly with cumulative rainfall (Fig. 3). Linear regression between individual gross rainfall and individual stemflow was:

$$\mathrm{SF}_C = 0.151P_\mathrm{G} - 0.3346 \quad (R^2 = 0.913, p < 0.001) \tag{4}$$

where P_G is the gross rainfall (mm), SF_C is the stemflow from *C. korshinskii* plant (mm). Rainfall threshold for stemflow generation was 2.2 mm according to linear regression for *C. korshinskii*. Stemflow accounted for 7.9±4.9% (Mean±SD) of rainfall and average funnelling ratio was 89.8 ranging from 6.4 to 168.5 (Fig. 4). Funnelling ratio was close to 60 when rainfall was less than 6 mm and close to 120 when rainfall was larger than 6 mm. There was a great variability in funnelling ratio when rainfall intensity was less than 6 mmh^{-1}. When rainfall intensity was greater than 6 mmh^{-1}, funnelling ratio tended to be stable with increasing rainfall intensity (Fig. 5).

3.3 Advance of wetting front

The wetting front was determined by evaluating the difference in soil moisture content for consecutive soil layers. The change in soil moisture with time from 20:00 LT, 28 August, to 20:00 LT, 7 September, and 17:00 LT, 22 September, to 17:00 LT, 7 October, is shown in Figs. 6 and 7. As seen from the figures, infiltrated water reached deeper soil depths after several hours from start of individual rainfall events. At depths greater than 30 cm, the change of soil moisture often lagged 20–24 h behind that of the top soil profile. For a consecutive series of large rainfall events with cumulative rainfall of 42.5 mm (from 0:00 LT of 22 September to 21:00 LT of 26 September), the wetting front reached a depth of 90 cm. For a consecutive series of small rainfall events with a cumulative rainfall of 11.3 mm (from 14:00 LT of 28 August to 7:00 LT of 29 August), the wetting front could not be noticed at a depth of 40 cm. The increase of soil moisture at the top layer 0–10 cm occurred at exactly the same time as the start of rainfall. The soil moisture in the upper soil profile fluctuated with the variation of rainfall intensity (Figs. 2, 6, and 7). However, there were no noticeable changes in soil moisture at the top soil profile for small-sized rainfall events at 72 and 261 h (Fig. 7). The soil moisture at the top layer of less than 20 cm declined quickly with the cessation of rainfall, though at 30 cm it declined slowly from a relatively large value. A similar trend is seen for soil moisture changes at soil depths larger than 30 cm, soil moisture increased to a maximum after rainfall events, and then declined slowly. Changes in soil moisture after rainfall were generally only noticed at depths of 0–55 cm.

The rainfall amount was compared with the total change of soil moisture at consecutive depths in the 0–55 cm soil (Table 2). For small-sized rainfall event (about 2.0 mm), no soil moisture change was observed. However, there was a clear increase in soil water when a small-sized rainfall event followed a larger rainfall event (e.g., 23 September). Medium-sized rainfall events (about 4 mm) could effectively infiltrate the soil profile and affected the cumulative infiltration at shallow soil layers. Also, the total soil moisture increase almost equaled to the corresponding rainfall amount. Under relatively large rainfall (about 14 mm), the soil moisture increase was greater than the corresponding rainfall amount.

4 Discussion

The experiments were done on eight *C. korshinskii* shrubs with plenty of branches that varied from 8 to 20 averaging 13 for each shrub (Table 1). The stem traits such as the diameter, length and the stretch angles of the branches together with the canopy projection were identical with typical mature *C. korshinskii* shrubs in the study area (Wang et al., 2005). The angle of the upward branches to the ground surface that averaged around 65° classified the shrub shape approximately to an inverted cone characterized by a relatively uniform upward branch stretch orientation (Table 1), indicating the applicable methodology for stemflow measurement was used in the present study.

For *C. korshinskii*, rainfall of at least 2.2 mm was necessary to initiate stemflow according to linear regression. This threshold is consistent with thresholds reported by previous studies in arid areas (e.g., Martinez-Meza and Whitford, 1996; Návar, 1993; Enright, 1987; Li et al., 2008). Stemflow accounted for 7.9% of the gross rainfall and the average funneling ratio was 89.8. For large rainfall events (>10 mm), stemflow concentrated more water to the root zone. Thus, the efficiency of water infiltration in soil is enhanced and soil moisture increase is larger than the corresponding rainfall.

Funneling ratio varied greatly for different rainfall events, depending upon the rainfall amount and rainfall intensity. Funneling ratios have been found to be greater than 10, and in some cases, far greater than 10 (e.g., Návar, 1993; Carlyle-Moses, 2004; Li et al., 2008). Our studies showed that there can be ten or even hundred times the rainwater amount that may reach the root area by stemflow as compared to an open area. The excess water effectively enhances the moisture of the upper soil layer, and then a greater water potential gradient is formed between the upper wet soil layer and the deeper dry soil profile. Consequently, the probability of water infiltrating to the deeper soil becomes higher around shrub stems. Also, stemflow water in desert shrubs may be assumed to be distributed to deep soil layer by preferential flow along root channels (e.g., Martinez-Meza and Whitford, 1996). For relatively large cumulative rainfall of 42.5 mm (from 00:00 LT of 22 September to 21:00 LT of 26 September), the wetting front reached a depth of 90 cm (Fig. 7). Hence, stemflow efficiently helps water to infiltrate to deeper soil layers that can be effectively utilized by the shrub plants.

Stemflow water can effectively refill the soil profile and increase the cumulative infiltration for medium- and large-sized rainfall. According to previous research, from the point view of soil moisture replenishment in this particular artificially re-vegetated sand dune area, only when an individual rainfall event has a rainfall amount >8 mm (Chen, 1991; Zhao, 1991), with average rainfall intensity >0.5 mm h^{-1} (Wang et al., 2008), it is an effective rainfall for the vegetated soil. While for the stem basal area of *C. korshinskii*, the corresponding threshold value is about 4 mm (Table 2, on 23 September

2008) which replenish the soil moisture at the profile deeper than 5 cm, comparing to the rainfall of 3.5 mm that limited the soil moisture increment within the upper layer of 5 cm (Table 2, on 3 October 2008). Therefore, stemflow doubled the effective rainfall in terms of the soil moisture replenishment in the root zone below 5 cm depth. Stemflow inputs depend not only on rainfall characteristics (such as rainfall amount, intensity, and duration), but also on meteorological conditions, seasonality, and canopy structure. On the other hand, there are interspecific and intraspecific differences among and within shrub species (e.g., Levia and Frost, 2003; Llorens and Domingo, 2007). Infiltration is also influenced by soil surface characteristics (such as microtopography, cracking, surface sealing, and crusting), soil physical properties (such as bulk density, organic matter and particle size distribution), and characteristics of the vegetation (such as plant biomass and cover) (e.g., Eldridge et al., 2000). For our study area, the fate of stemflow is probably mainly affected by the properties of the biological soil crust formation that develops around the shrub stems. From our studies we can conclude that it is important to quantify the stemflow when designing shrub plantations in arid areas. Stemflow contributes efficiently to the water availability for the plant roots. Consequently, stemflow is an important part of the local water balance around shrub species.

5 Conclusions

A better understanding of the stemflow variability and its contribution to soil moisture is essential in the re-vegetation efforts of inhabited arid regions. An antecedent precipitation of 2.2 mm is needed for the initiation of stemflow of the shrub stand. Owing to the high values of funneling ratio (e.g., 90) of the studied species, the shrub plants can concentrate water flux to the stem basal area. A threshold value of corresponding rainfall of 4 mm is required for stemflow water to replenish the soil moisture at the stem basal area. Thus, from the point view of funneling ratio and cumulative infiltration, we may conclude that especially for the studied area, where rainfall events typically are small and of low intensity, stemflow is of immense importance to sustain the ecosystem close to and around shrubs at the stand scale.

Acknowledgement. The experiment is jointly supported by the CAS Action Plan for West Development Program (KZCX2-XB2-09), the National Natural Science Foundation of China (40871051) and the Western (China) Lightening Foundation of the Talent Training Program of Chinese Academy of Sciences. This publication has been produced during xpw's scholarship period at Lund University thanks to a Swedish Institute scholarship.

References

Berndtsson, R., Nodomi, K., Yasuda, H., Persson, T., Chen, H., and Jinno, K.: Soil water and temperature patterns in an arid desert dune sand, J. Hydrol., 185, 221–240, 1996.

Carlyle-Moses, D. E.: Throughfall, stemflow, and canopy interception loss fluxes in a semi-arid Sierra Madre Oriental matorral community, J. Arid Environ., 58, 181–202, 2004.

Chen, W. R.: Water balance in the revegetated area along the railway in Shapotou area, in: Study on Shifting Sand Control in Shapotou Region of the Tengger Desert (2), edited by: Shapotou Desert Experimental Research Station, Chinese Academy of Sciences, Ningxia People's Publishing House, Yinchuan, 66–75, 1991.

Dunkerley, D.: Identifying individual rain events from pluviograph records: a review with analysis of data from an Australian dryland site, Hydrol. Process., 22, 5024–5036, 2008.

Eldridge, D. J., Zaady, E., and Shachak, M.: Infiltration through three contrasting biological soil crusts in patterned landscape in the Negev, Israel, Catena, 40, 323–336, 2000.

Enright, N. J.: Stemflow as a nutrient source for nikau palm (*Rhopalostylis sapida*) in a New Zealand forest, Aust. J. Ecol., 12, 17–24, 1987.

Herwitz, S. R.: Infiltration-excess caused by stemflow in a cyclone-prone tropical rainforest, Earth Surf. Proc. Land, 11, 401–412, 1986.

Levia, D. F. and Frost, E. E.: A review and evaluation of stemflow literature in the hydrologic and biogeochemical cycles of froested and agricultural ecosystems, J. Hydrol., 274 (1–4), 1–29, 2003.

Li, X. Y., Liu, L. Y., Gao, S. Y., Ma, Y. J., and Yang, Z. P.: Stemflow in three shrubs and its effect on soil water enhancement in semiarid loess region of China, Agric. Forest Meteorol., 148(10), 1501–1507, 2008.

Llorens, P. and Domingo, F.: Rainfall partitioning by vegetation under Mediterranean conditions. A review of studies in Europe, J. Hydrol., 335, 37–54, 2007.

Martinez-Meza, E. and Whitford, W. G.: Stemflow, throughfall and channelization of stemflow by roots in three Chihuahuan desert shrubs, J. Arid Environ., 32, 271–287, 1996.

Návar, J.: The causes of stemflow variation in three semiarid growing species of Northeastern Mexico, J. Hydrol., 145, 165–190, 1993.

Návar, J. and Bryan, R. B.: Interception loss and rainfall redistribution by three semi-arid growing shrubs in Northeastern Mexico, J. Hydrol., 115, 51–63, 1990.

Noborio, K., McInnes, K. J., and Heilman, J. L.: Measurements of cumulative infiltration and wetting front location by time domain reflectometry, Soil Sci., 161, 480–483, 1996.

Nulsen, R. A., Bligh, K. J., Baxter, I. N., Solin, E. J., and Imrie, D. H.: The fate of rainfall in a mallee and heath vegetated catchment in Southern Western Australia, Aust. J. Ecol., 11, 361–371, 1986.

Pressland, A. J.: Soil moisture redistribution as affected by throughfall and stemflow in an arid zone shrub community, Aust. J. Bot., 24, 641–649, 1976.

Tromble, J. M.: Water interception by two arid land shrubs, J. Arid Environ., 15, 65–70, 1987.

Vörösmarty, C. j., Green, P., Salisbury, J., and Lammers, R. B.: Global water resources: vulnerability from climate change and population growth, Science, 289, 284–288, 2000.

Wang, X. P., Cui, Y., Pan, Y. X., Li. X. R., Yu, Z., and Young, M. H.: Effects of rainfall characteristics on infiltration and redistribution patterns in revegetation-stabilized desert ecosystems, J. Hydrol., 358, 134–143, 2008.

Wang, X. P., Li, X. R., Zhang, J. G., Zhang, Z. S., and Berndtsson, R.: Measurement of rainfall interception by xerophytic shrubs in re-vegetated sand dunes, Hydrol. Sci. J., 50, 897–910, 2005.

Wang, X. P., Li, X. R., Xiao, H. L., Berndtsson, R., and Pan, Y. X.: Effects of surface characteristics on infiltration patterns in an arid shrub desert, Hydrol. Process., 21, 72–79, 2007.

Zhao, X. L.: Problems of revegetation on sand dunes in Shapotou area, in: Study on Shifting Sand Control in Shapotou Region of the Tengger Desert (2), edited by: Shapotou Desert Experimental Research Station, Chinese Academy of Sciences, Ningxia People's Publishing House, Yinchuan, 27–57, 1991.

Table 1. Desrciptive statistics (mean ± standard deviation) of branches and canopy projection of the *C. corshinskii* shrubs used in the experiments.

			Shrub branch			Canopy projection
	Number	Diameter (cm)	Length (cm)	Height (cm)	Angle (°)[a]	(cm^2)
Shrub 1	20	1.6±0.2	184±11.1	51.4±32.0	62.0±18.0	80 425
Shrub 2	11	2.0±0.3	223±38.0	72.0±16.4	65.9±4.5	28 274
Shrub 3	10	1.6±0.7	138±30.6	43.3±12.1	63.8±8.8	22 619
Shrub 4	14	2.0±0.8	145±21.8	36.0±18.2	52.2±19.5	52 779
Shrub 5	20	2.0±0.8	176±26.1	52.0±13.0	66.7±4.5	45 239
Shrub 6	8	1.4±0.4	158±27.4	40.0±14.1	69.0±11.6	20 028
Shrub 7	6	2.2±0.6	206±18.2	37.0±19.2	75.4±11.0	28 353
Shrub 8	14	1.3±0.3	126±5.5	30.0±18.7	65.8±22.8	17 868
Average	**13**	**1.8±0.3**	**170±34**	**45.2±13.2**	**65.1±6.6**	**36 948±21 429**

[a] Angle in degree of the upward branch to the ground surface.

Table 2. Changes in cumulative infiltration (mm) at different soil layers.

	29 Aug	8 Sep	9 Sep	23 Sep	25 Sep	26 Sep	3 Oct
Rainfall (mm)	7.9	1.6	2.0	4.0	7.5	14.0	3.5
Layer 0–5 cm	1.75	0	0	0.40	1.65	1.60	0.05
Layer 5–10 cm	2.15	0	0	0.40	1.40	1.80	0
Layer 10–15 cm	1.95	0	0	0.55	1.05	1.85	0
Layer 15–20 cm	1.00	0	0	0.15	0.75	1.70	0
Layer 20–25 cm	0.85	0	0	0.30	0.45	1.95	0
Layer 25–30 cm	0.30	0	0	0.30	0.30	1.70	0
Layer 35–40 cm	0	0	0	0.50	0.15	1.95	0
Layer 40–45 cm	0	0	0	0	0.05	2.85	0
Layer 45–50 cm	0	0	0	0	0	2.60	0
Layer 50–55 cm	0	0	0	0	0	1.25	0
Soil moisture increase (mm)	8.00	0	0	2.60	5.80	19.25	0.05

Fig. 1. Photographs showing method of collecting stemflow for *C. korshinskii*.

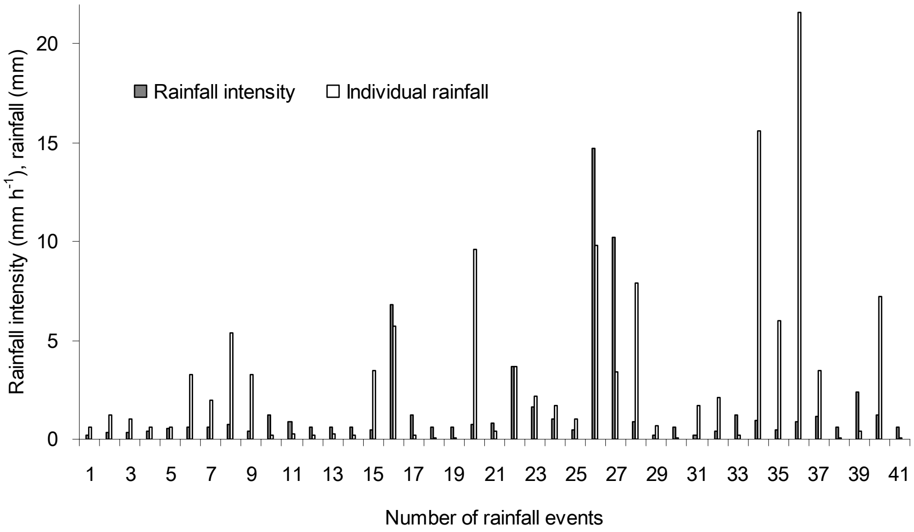

Fig. 2. Rainfall intensity and individual rainfall of the total 41 rainfall events in the year 2008 at the experimental site.

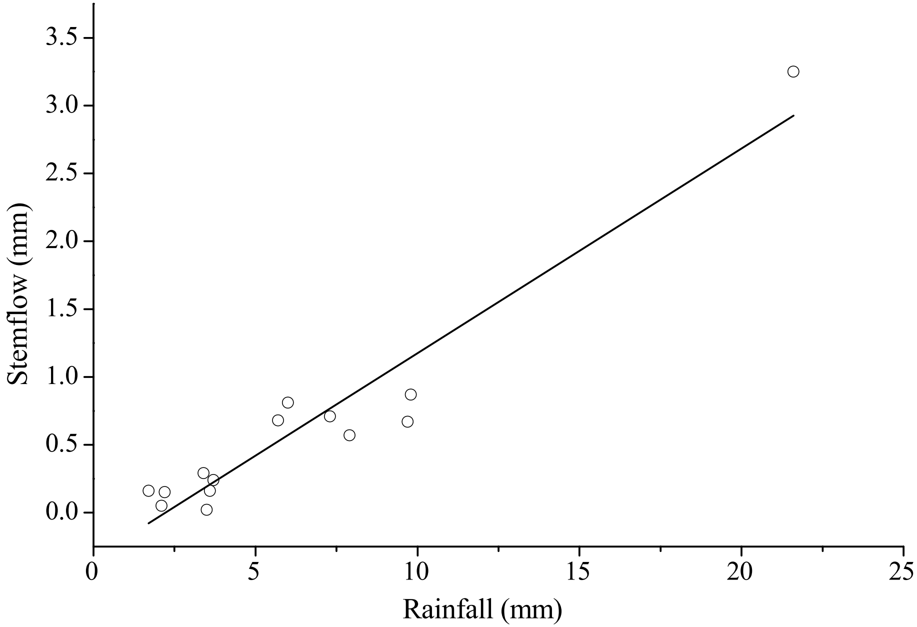

Fig. 3. Relationship between individual rainfall and stemflow for *C. korshinskii*.

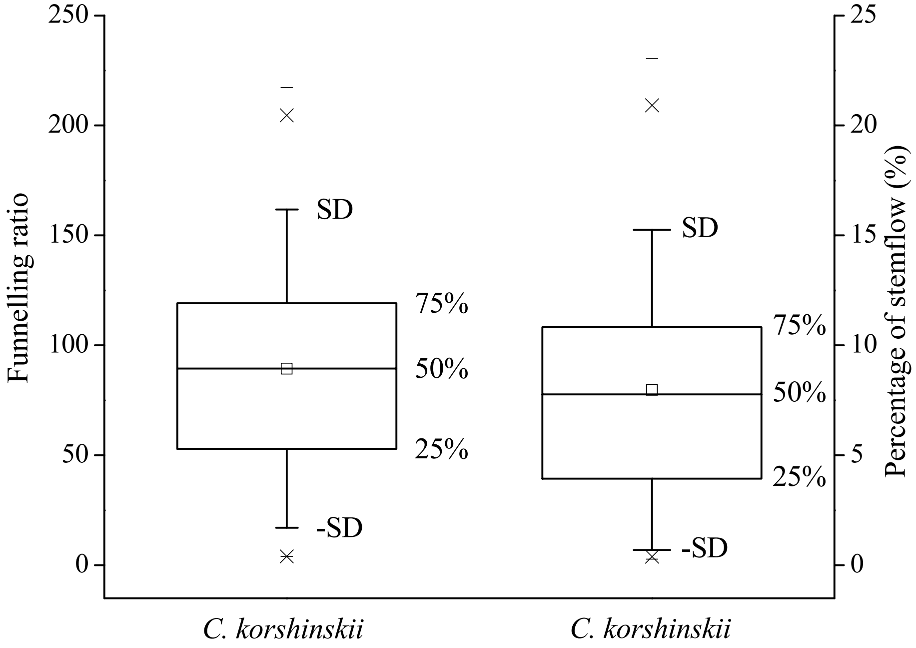

Fig. 4. Box-and-whisker diagrams showing median, 25, 50, 75 percentiles, and standard deviation for individual funneling ratio and stemflow percentage for *C. korshinskii*. (☐) represents mean value, (–) maximum and minimum value and (×) are 1st and 99th percentiles.

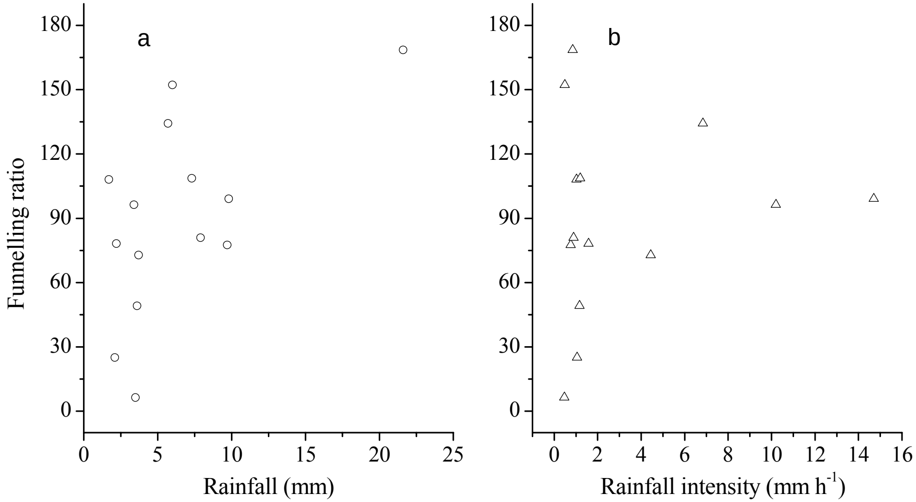

Fig. 5. Relationship between funnelling ratio and rainfall amount **(a)** and rainfall intensity **(b)**.

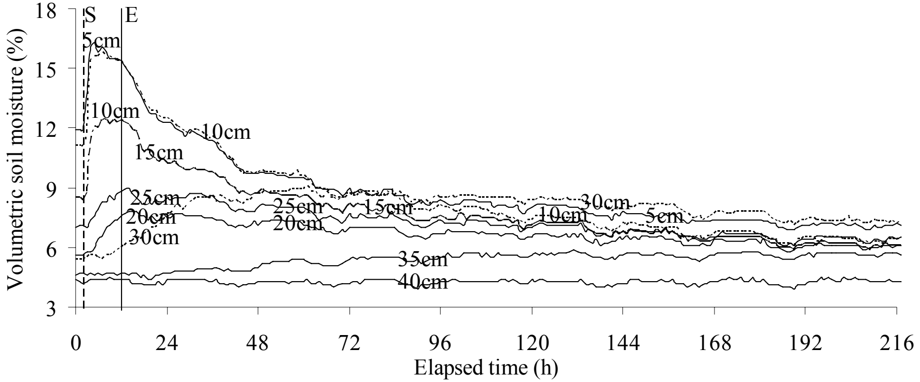

Fig. 6. The wetting front advance from 20:00 LT of 28 August to 20:00 LT of 7 September (S) represents the start of rainfall, (E) the end of rainfall.

Title Page
Abstract
Introduction
Conclusions
References
Tables
Figures
◂
▸
Back
Close
Full Screen / Esc
Printer-friendly Version
Interactive Discussion

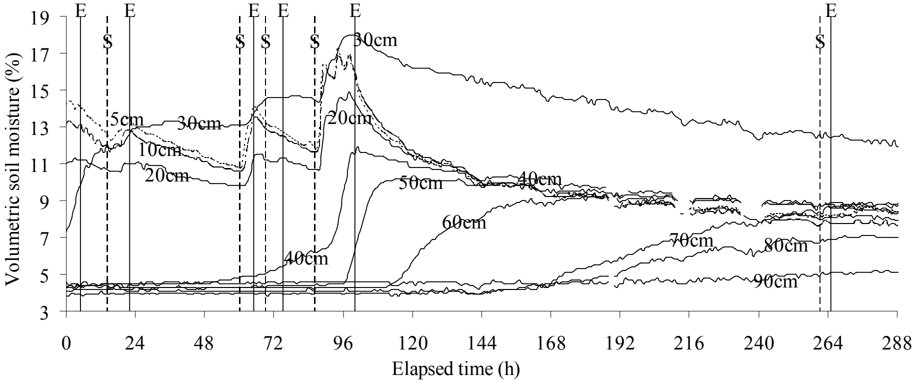

Fig. 7. The wetting front advance from 17:00 LT of 22 September to 17:00 LT of 7 October (S) represents the start of rainfall, (E) the end of rainfall.